UC San Diego

UC San Diego Electronic Theses and Dissertations

Title

Impact of temporal resolution on demand charge reduction using real-time model based predictive control of a battery energy storage system (BESS)

Permalink

https://escholarship.org/uc/item/0zc1g0v4

Author

Roy, Rahul

Publication Date

2022

Peer reviewed|Thesis/dissertation

eScholarship.org Powered by the California Digital Library
University of California

UNIVERSITY OF CALIFORNIA SAN DIEGO

Impact of temporal resolution on demand charge reduction using real-time model based predictive control of a battery energy storage system (BESS)

A thesis submitted in partial satisfaction of the
requirements for the degree
Master of Science

in

Engineering Sciences (Mechanical Engineering)

by

Rahul Roy

Committee in charge:

Professor Jan Kleissl, Chair
Professor Patricia Hidalgo-Gonzalez
Professor Yuanyuan Shi

2022

Copyright

Rahul Roy, 2022

All rights reserved.

The thesis of Rahul Roy is approved, and it is acceptable in quality and form for publication on microfilm and electronically.

University of California San Diego

2022

DEDICATION

This thesis work is dedicated to my parents, Chandranath and Sucheta Roy, who have been a constant support and encouragement during the challenges of graduate school and life. They have always always loved me unconditionally and whose good examples have taught me to work hard for the things that I aspire to achieve.

TABLE OF CONTENTS

LIST OF FIGURES

ACKNOWLEDGEMENTS

I would like to acknowledge Professor Jan Kleissl for his support as the chair of my committee. Through multiple drafts and discussions, his invaluable guidance leads me to the right path. I would also like to acknowledge Doctor Sushil Silwal from CER, UCSD, without whom the journey of this research would be more tough.

The thesis is currently being prepared for submission for publication of the material. Roy, Rahul; Silwal, Sushil; Kleissl, Jan. The thesis author was the primary investigator and author of this material.

ABSTRACT OF THE THESIS

Impact of temporal resolution on demand charge reduction using real-time model based predictive control of a battery energy storage system (BESS)

by

Rahul Roy

Master of Science in Engineering Sciences (Mechanical Engineering)

University of California San Diego, 2022

Professor Jan Kleissl, Chair

Grid-connected battery energy storage systems (BESS) are a promising technology to decrease peak load. In this paper, a linear programming (LP) optimization model of a BESS that minimizes demand charge in real-time is developed. The model is employed to study the effect of two temporal resolutions of load profiles, 15 min and 1 hour, on peak load shaving and optimal sizing of BESS. In contrast to previous studies with perfect forecast, realistic forecast errors are prescribed; a 24 hour persistence forecasts and a recurrent neural network (RNN) model are used for short-term load forecasts. The LP routine was coupled with model predictive control (MPC) to obtain optimal BESS dispatch schedules and to reduce the deviations due to load forecast

errors in real time. The performance of the proposed algorithm is simulated for one month on a grid-connected building. Compared to perfect load forecasts, the RNN forecast error causes a monthly average of 1.3 kW higher optimized net load, and corresponding $27 higher optimal demand charge (ODC). Correcting persistence forecast with more accurate RNN forecast yield better peak shaving performance with a monthly average of 28.1% reduction in optimized net load. The temporal load resolution has a significant influence on the ODC. The difference of ODC for two temporal resolutions depend strongly on the load profile characteristics. When the battery capacity is above a certain power and energy threshold limit, the 1 hour load profile is found to be sufficient for determining ODC. However, when the power and/or energy is constrained, the difference in the ODC between 15 min and 1 hour resolution ranges from $14.7 to $123.1 for 28 days.

Chapter 1

INTRODUCTION

1.1 Literature Review

In recent years, there has been a significant research interest in using grid-connected battery energy storage systems (BESS) for demand charge reduction. BESS can reduce electricity costs in commercial buildings by discharging stored energy during peak loads [31]. Ehsan et al. [35] implemented nonlinear programming to charge or discharge a BESS based on daily load forecasts. Lavrova et al. [18] analyzed the cost effectiveness of BESS in terms of power smoothing, peak load shaving, and other ancillary services. The economic feasibility of BESSs depends on three parameters; the difference between high and low electricity prices, peak demand charge, and investment cost for BESS [38]. Dejvises et al. [9] applied a mathematical model to simulate BESS operation, reducing daily electrical peak power demand by 7.4% with a 9.9% increase of daily load factor. Successful peak shaving strategy requires optimal operation of the BESS. Some studies considered simple rule-based optimization to charge the battery at low demand and discharge at peak demand [47, 24, 19, 35]. Chua et al. [7] used a rule-based adaptive control algorithm to determine the optimum operation of BESSs. Rahimi et al. [34] developed a controller for demand charge reduction that operated the battery based on short term load forecasted load. Additional research on the optimum operation of BESSs for peak shaving applications can be found in [6, 13, 40, 16].

BESS size was optimized by evaluating the energy capacity required to meet the peak

load demand based on daily forecasted load[23] and historical load profiles[7]. Thongchart et al. [15] used particle swam optimization to determine the optimal size of BESS at minimal total BESS cost. Many research works have optimized the battery size to balance the BESS installation cost and electricity bill savings [39, 30, 21, 2, 28, 41, 27, 14]. Hassan et al. [11] analyzed the impact of BESS unit cost on its adoption using the Distributed Energy Resources Customer Adoption Model (DER-CAM) software.

Many authors employed modeling approaches and forecast-based strategies for optimized operation of photovoltaic-battery (PVB) systems, such as linear [8] and mixed integer-linear programming [33], dynamic programming [36], neural networks [26] as well as model predictive control [17] (MPC). [3, 44] considered a PV and load forecast-based control strategy to operate the BESS. Researchers used MPC as a supervisory layer for optimal operation of the BESS [25]. Wu et al. [42] scheduled a grid-connected PVB system in real time using MPC. Zhang et al. [45] showed that MPC performs better in minimizing operation costs of microgrids under different forecast uncertainty levels of load demand, electricity cost, and renewable generation than other scheduling and operation strategies. MPC was applied for energy management in microgrids by [32, 46].

The operation of BESS for peak load shaving is sensitive to the temporal resolution of the load profiles. Most publicly available databases for weather data and load profiles are based on a 1 hour resolution [12]. Cao and Siren [5] showed that a 1 hour time resolution can cause significant errors in the matching of photovoltaic (PV) generation and household electric demand. Beck et al. [1] concluded that load resolution has a significant impact on optimal sizing of PVB systems when maximizing the revenue from feed-in tariffs. A similar conclusion was drawn by Wyrsch et al. [43] who considered 6 s measured load resolution data and averaged it to 1 hour to match it with PV generation data. Longer time averaging of supply and demand profiles leads to significant overestimation of direct self-consumption, degree of autarky and battery lifetime [37]. Burgio at al. [4] showed that for a PVB system, the peak load of one day decreased 39.4% from 52 kW to 32 kW as the time resolution changed from 3 min to 1 hour.

Liu et al. [22] studied the impact of temporal load resolution on demand charge reduction for perfect forecasts for a large range of BESS energy and power capacities. Hourly load profiles significantly underestimated the optimal demand charge (compared to 15 min load profiles) when the power or energy capacity of the BESS is constrained below certain critical limits.

1.2 Objectives and Contribution

Following Liu et al.[22], the goal of our research is to study demand charge reduction for high (15 min) and low (1 hour) temporal load resolutions in real-time. Rather than using perfect load forecasts [22], we adopt a MPC-based linear program (LP) optimal BESS dispatch strategy using two short-term load forecasts with different levels of realistic forecast errors: 24 hour persistence forecast and 24 hour load forecast based on a recurrent neural network (RNN) model. This corrective optimization framework replicates the real-world feature of better prediction accuracy with a reduced forecast horizon. This allows us to study the effect of different load forecasting models on the optimum demand charge.

MPC optimizes the operation of the BESS by solving an LP problem at every time step. In real-time the BESS dispatch is adjusted for disparities between the prediction and demand load measurement. As a case study, we tested our model with real load data from a police building.The impact of temporal resolution on peak shaving is quantified as the deviation of optimized demand charge at 1 hour versus 15 min load resolution for different BESS power and energy ratings. The main novelties are:

1. Quantifying the impact of temporal load resolution on demand charge reduction using BESS operation considering *real-time load data*.

2. Quantifying how characteristics of short-term load forecasts affect the demand charge reduction.

1.3 Paper Organisation

The remainder of this paper is divided into four sections. The proposed LP optimization model for minimizing demand charge along with the BESS constraints is described in Section 2.1. We introduce the load forecasts, model predictive control algorithm and the battery parameters in Sections 2.2, 2.3 and 2.4 respectively. The data is described in Section 2.5. Section 3.1 and Section 3.2 presents the demand charge simulation results on a sample day, as well one month of operations respectively. The effect of temporal resolution on demand charges is compared across a ratings space defined by BESS power and energy capacity in Section 3.3. Lastly, Section 4 completes the paper with concluding remarks and recommendations for future work.

Chapter 2

SYSTEM MODELING

2.1 Linear optimization model

A linear programming model is written in MATLAB CVX with MOSEK as a solver for the convex optimization problem, which is designed in discrete time intervals, Δt, based on the temporal resolution of the electrical load profile. The setup and equation in this section are identical to Liu et al. [22]. The optimization model calculates the optimal power flows between the BESS, electrical grid, and the building load (Fig. 2.1). The electricity imported by the grid (P_g) is offset by the charging/discharging (P_b) of the BESS to meet the load (l) in real time. The present work is also applicable to PVB systems, where the load is replaced by the summation of actual load and PV generation.

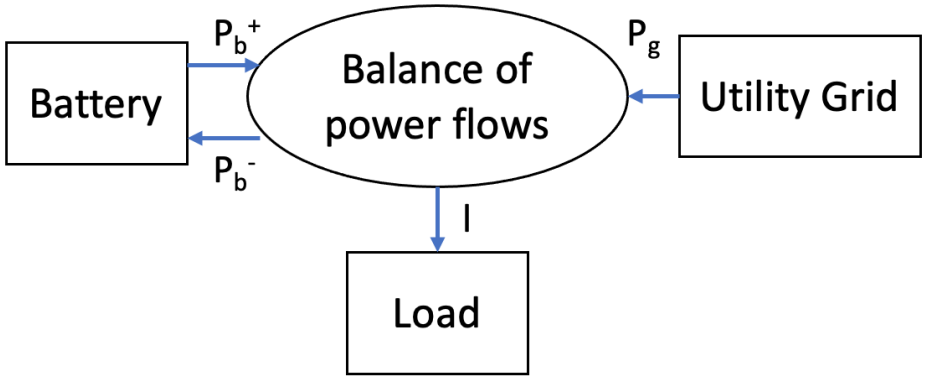

Figure 2.1. Schematic diagram of the grid-connected battery energy storage system, the load, and the utility grid.

The target of the optimization is the minimization of the peak demand charge. The objective function is

$$\min(\text{obj}) = \text{d} \times \max(\text{P}_\text{g}) + \varepsilon \times \sum_{\text{t}=0}^{\text{T}} |\text{P}_\text{b}^\text{t}| \tag{2.1}$$

where t is the time index and T is the total number of time intervals. The objective function consists of the optimal demand charge (ODC) and a penalty term

$$\text{ODC} = \text{d} \times \max(\text{P}_\text{g}) = \text{d} \times \text{OP}, \tag{2.2}$$

where d is the demand charge rate, set at a constant value of \$20.62, obtained from the AL-TOU rate schedule by San Diego Gas & Electric (SDG&E) utility company. The optimal peak (OP) is the maximum net load during the day. The second term in Eq. 2.1 ensures the optimal demand charge solution with the least battery activity by multiplying a small penalty factor $\varepsilon = 10^{-6}$ into the battery charging/discharging oscillations.

The following assumptions are considered:

1. All the electronic interfaces of the utility grid, load and BESS are assumed to be 100% efficient.

2. The charging and discharging of the battery are assumed to be 100% efficient.

3. The system energy conversion and transmission are perfectly efficient.

4. As Lithium-ion batteries have a response time on the order of milliseconds, the BESS charging/discharging dispatch is assumed to be instantaneous [29].

5. The loss of stored electricity due to the self-discharge rate of the battery is neglected as it is small (0.1%/day) [20]

The main constraint of the optimization model is the load balance equation, which ensures

that the load l^t of the building is satisfied by the grid P_g^t and battery P_b^t at all times.

$$P_g^t + P_b^t = l^t, \quad \forall t \in T \tag{2.3}$$

The BESS is modeled according to Eq. 2.4. The energy conservation at every time interval of the battery is accounted for in Eq. 2.4a, where the state of charge (SOC) is defined as the ratio between stored electrical energy and the rated battery capacity c_e. The power flows entering and exiting the battery are constrained by the power capacity c_p as shown in Eq. 2.4b. The discharging or charging of the battery is denoted by positive or negative values of P_b, respectively. According to Eq. 2.4c, the SOC is retained at 0.5 during the beginning and end of the simulation period. Therefore, savings through energy sales are avoided as the net charging/discharging energy of the battery is zero. The SOC is always kept within the minimum and maximum limits of the battery (Eq. 2.4e).

$$SOC^{t+1} = SOC^t - \frac{P_b^t \times (\Delta t)}{c_e}, \quad \forall t \in T \tag{2.4a}$$

$$-c_p \leq P_b^t \leq c_p, \quad \forall t \in T \tag{2.4b}$$

$$SOC^{start} = SOC^{end} = 0.5 \tag{2.4c}$$

$$SOC^{min} \leq SOC^t \leq SOC^{max} \tag{2.4d}$$

$$SOC^{min} = 0; SOC^{max} = 1 \tag{2.4e}$$

2.2 Load forecasting

We consider three different 24 hour ahead load forecasts representing different forecast accuracies.

1. *Perfect Forecast*: The entire 24 hour horizon consists of the actual load profile, yielding zero forecast error. Therefore Steps 4 through 6 in Fig. 2.2 are not needed. The perfect forecast represents the maximum peak load shaving achievable by the BESS. With sufficient battery capacity, the perfect forecast would yield a flat net load curve [22].

2. *Base or Persistence Forecast*: As a standard benchmark for load forecasting, the 24 hour persistence forecast is characterized as the load at the same 15 min time step of the previous day[10]. Persistence forecast are separated into weekdays and weekends. For example, persistence from the preceding Fridays is assumed for Mondays and for Saturdays, we consider load from the preceding Sunday. The 24-hour persistence forecast has the largest forecast error.

3. *Operational or RNN Forecast*: Trained on the previous year of load, we use a recurrent neural network (RNN) model to predict the 24 hour load. The RNN forecast is typically more accurate than the persistence forecast.

2.3 Model Predictive Control (MPC)

MPC is a receding horizon optimization-based control method. The basic concept of MPC is that at each time step, a look-ahead finite-horizon optimal control problem is solved but only the first step of the control sequences is implemented. The time-domain trajectory of state variables over the prediction horizon is described by a predictive model, with the initial state being the measured state of the actual system. After the implementation of the first step, the system waits until the next step. At the next step, with a new measurement, the optimal control routine is computed again. The optimal control problem is formulated for peak demand shaving based on MPC as follows (Fig. 2.2):

1. Set the time step t at the beginning of the simulation period equal to zero i.e. $t = 0$.

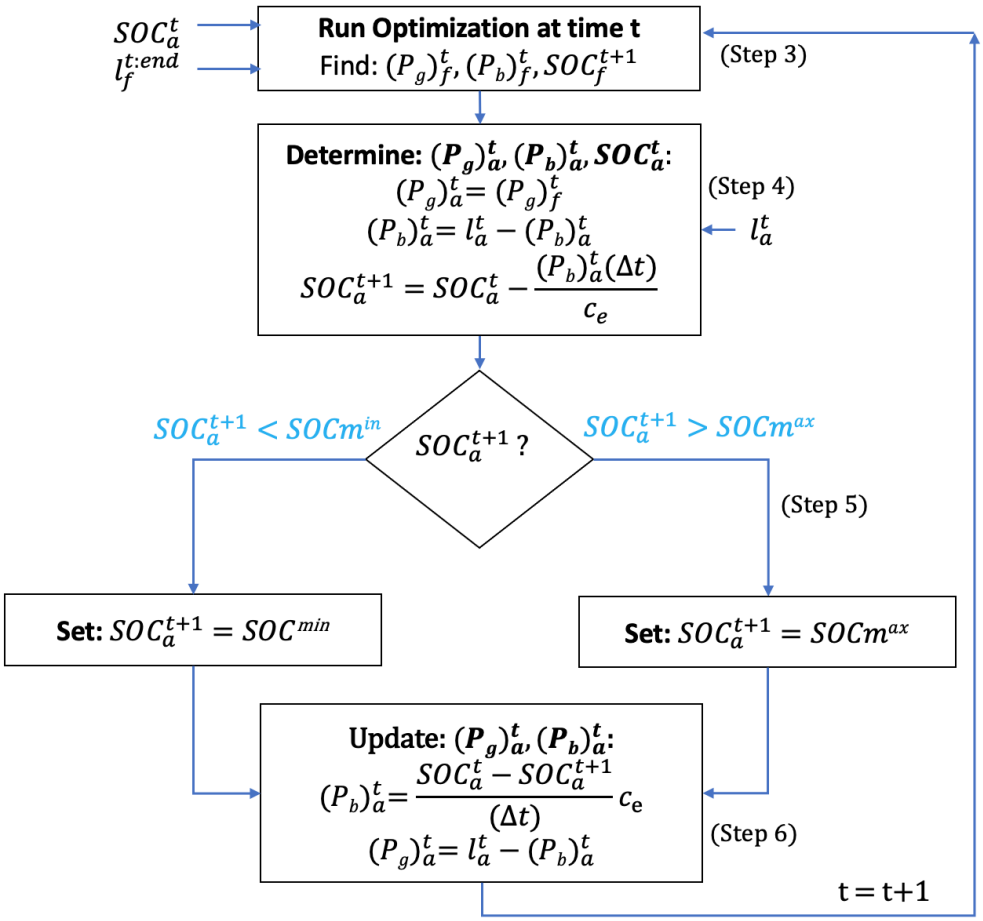

Figure 2.2. Flow chart illustrating the model predictive control algorithm in the battery dispatch schedule for peak load shaving

2. Select a moving horizon of 24 hours discretized into either 15 min or 1 hour step sizes, i.e. $\Delta T = 0.25$ for 15 min and $\Delta T = 1$ for 1 hour. Load the forecasted load data for the entire receding horizon.

3. Solve the convex optimization problem that minimizes the objective function (Eq. 2.1) from the t-th interval for the entire 24 hour horizon to find the forecasted grid import $(\mathrm{P_g})_\mathrm{f}^\mathrm{t}$, battery output $(\mathrm{P_b})_\mathrm{f}^\mathrm{t}$ and SOC at the end of the t-th time interval $(\mathrm{SOC})_\mathrm{f}^{\mathrm{t+1}}$.

4. The actual grid import $(\mathrm{P_g})_\mathrm{a}^\mathrm{t}$ is determined by choosing the forecasted grid import from the previous step i.e. $(\mathrm{P_g})_\mathrm{a}^\mathrm{t} = (\mathrm{P_g})_\mathrm{f}^\mathrm{t}$. The battery output $(\mathrm{P_b})_\mathrm{a}^\mathrm{t}$ and SOC $(\mathrm{SOC})_\mathrm{a}^{\mathrm{t+1}}$ is adjusted

considering the actual load at the beginning of the t-th interval.

5. If SOC of the battery at time step t exceeds the allowed threshold limit, set the SOC to the boundary value (Eq. 2.4e).

6. First, adjust the actual battery output to compensate for real time forecast errors and then adjust the grid import accordingly. Set $t = t + 1$ and update the load data for the next control iteration. Go to step 2.

2.4 Battery space analysis

We consider two temporal resolutions of load data: 15 min and 1 hour, similar to Liu et al. [22]. The load is metered at 15 min intervals and is referred to as the reference load data. The coarse resolution (hourly) profile is derived by taking the average of four time steps. The hourly resolution is chosen as many data sets and optimization models for peak shaving are based on 1 hour resolution. The 15 min resolution optimization requires more computation time as it has 4 times the number of battery dispatch decisions compared to the 1 hour resolution. The 1 hour average load can result in different objective function values compared to the reference load, which can result in a different optimal demand charge. Following [22], the difference of demand charge (DODC) is defined as

$$\text{DODC} = \text{ODC}_{15-\text{min}} - \text{ODC}_{1-\text{hour}} \tag{2.5}$$

where ODC_{15-min} and ODC_{1-hour} are the optimal demand charge achieved with the load profiles at 15 min and 1 hour time resolution, respectively. DODC quantifies the peak shaving error that occurs when optimizing dispatch using loads at coarse temporal resolution. For a specific load profile, the DODC mainly depends on the BESS capacities, i.e. power capacity, c_p, and energy capacity, c_e. The optimum peak (OP) is defined as the maximum net load. For perfect forecasts, there exists an ideal c_p (critical power, CP) and c_e (critical energy, CE) that reduce the peak load

to the perfect peak (PP) i.e. average power of the daily load; further increase in battery capacities will not lower the maximum net load [22].

$$\mathrm{CP} = \max|l^t - \mathrm{PP}| \tag{2.6a}$$

$$\mathrm{CE} = 2 \times \max|\sum_{t=1}^{T}[(l^t - \mathrm{PP}) \times \Delta t]| \tag{2.6b}$$

CP measures the maximum distance from the time-varying load to the PP, whereas the CE is the maximum absolute value of the cumulative sum of the distance from the 15 min load to the PP for all time steps. We denote the critical power for 15 min and 1 hour load resolutions as $\mathrm{CP}_{15-\mathrm{min}}$ and $\mathrm{CP}_{1-\mathrm{hour}}$, respectively. The critical BESS capacities determine the critical point in the battery ratings space above which the DODC is exactly zero for perfect forecast.

2.5 Data

The input load data for this study was obtained from the Police building at the University of California, San Diego (UCSD). The Police building is a single story, 14,566 square foot building that was constructed in 1991. The electrical load profile was measured during September 2018 to February 2020 at a temporal resolution of 15 min and was quality controlled in [**?**]. In this paper only data for February 2020 is used. The load profile shows typical load variations for a commercial building.

Chapter 3

RESULTS AND DISCUSSION

3.1 Case study for a single day

The results are first shown for a single day, i.e. February 1, with the RNN forecast. According to Liu et al. [22], there is a significant difference in ODC when the power and/or energy capacity of the BESS are constrained below its critical capacities (Eq. 2.6b). Therefore, we have selected a BESS with a power capacity c_p = 8 kW and energy capacity c_e = 100 kWh. Per the BESS classification presented later in Section 3.3, this BESS is power constrained as the CP of Feb 1 is 10.4 kW. Fig. 3.1a shows the optimization results of the BESS. The net load is almost flat over the day but varies due to RNN load forecast errors and the power-constrained BESS. From the middle plot in Fig. 3.1a, we observe that the battery is charged to approximately 80% until 09:45 h before the peak load period starting at 11:45 h. The battery discharges until the evening at 18:00 to shave the grid profile towards the perfect peak. The BESS does not discharge completely as we have constrained the battery SOC at 50% at the end of the day. The maximum power imported from the grid is 34.37 kW (11:45 - 12:00) and 33.61 kW (00:00 - 01:00) for 15 min and 1 hour resolution respectively, which is close to the perfect peak (PP) value of 32.44 kW. The net loads are larger than the PP for two reasons: a) the power capacity of the battery is less than CP and b) the RNN forecasted load is higher than the actual load by 0.51 kW and 0.25 kW for 15 min and 1 hour load respectively.

Fig. 3.1a (bottom) shows that the power capacity of the BESS is fully utilized during

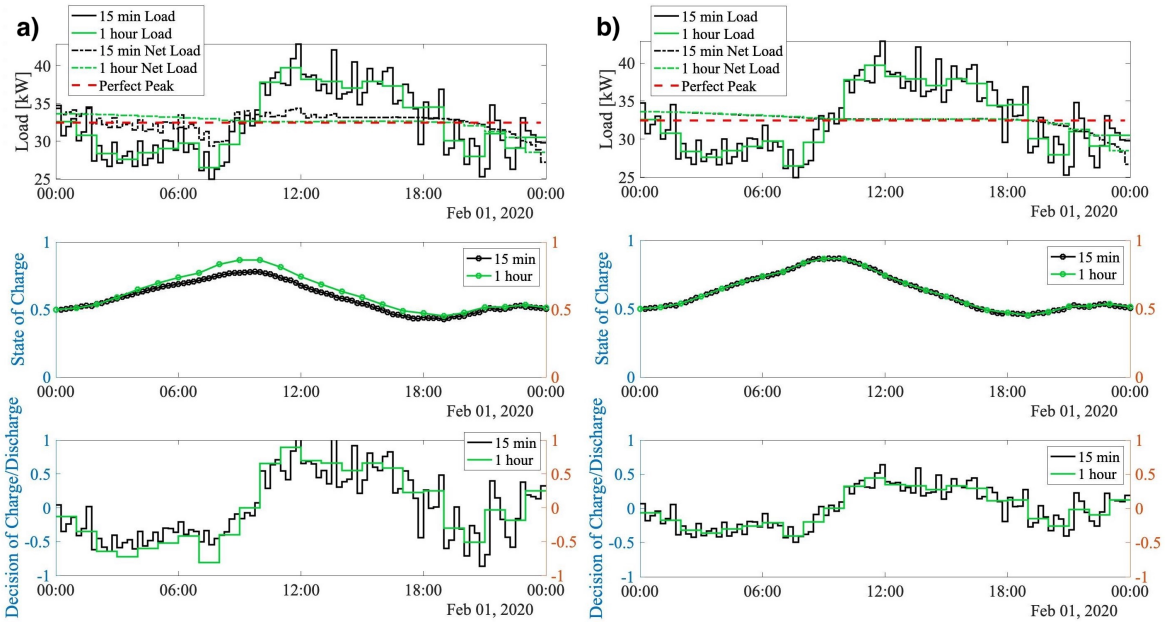

Figure 3.1. 15 min and 1 hour optimized net load (top), battery SOC (middle) and battery charging/discharging decision (bottom) on Feb 1, 2020 based on RNN forecast with BESSs of a) c_p = 8 kW and c_e = 100 kWh (power-constrained); b) c_p = 16 kW and c_e = 100 kWh ().

the 15 min time interval with peak demand (11:45 - 12:00). The demand charge is reduced by \$175.55, or 19.85% and \$125.78, or 15.36% of the maximum load profile value for 15 min and 1 hour resolution respectively. This significant reduction supports the potential of BESS for demand charge management. The 15 min net load is higher during the time interval 11:00 - 12:00 as the power capacity of the BESS is constrained at 8 kW. As the BESS power capacity is increased to 16 kW in Fig. 3.1b, we observe that the net load is completely flattened near the PP. The difference of demand charge (DODC) is \$15.6, i.e. the demand charge is underestimated by 2.2% compared to the 15 min temporal resolution. The results confirm that the 1 hour load profile will overestimate BESS peak load shaving.

As the predicted load is higher than the actual load during 00:00 to 09:00 (Fig. 3.2), the optimized net load is higher than PP during that interval in both plots. The additional power is used to further charge the BESS. Therefore, the load forecast error due to RNN model contributes significantly towards demand charge reduction.

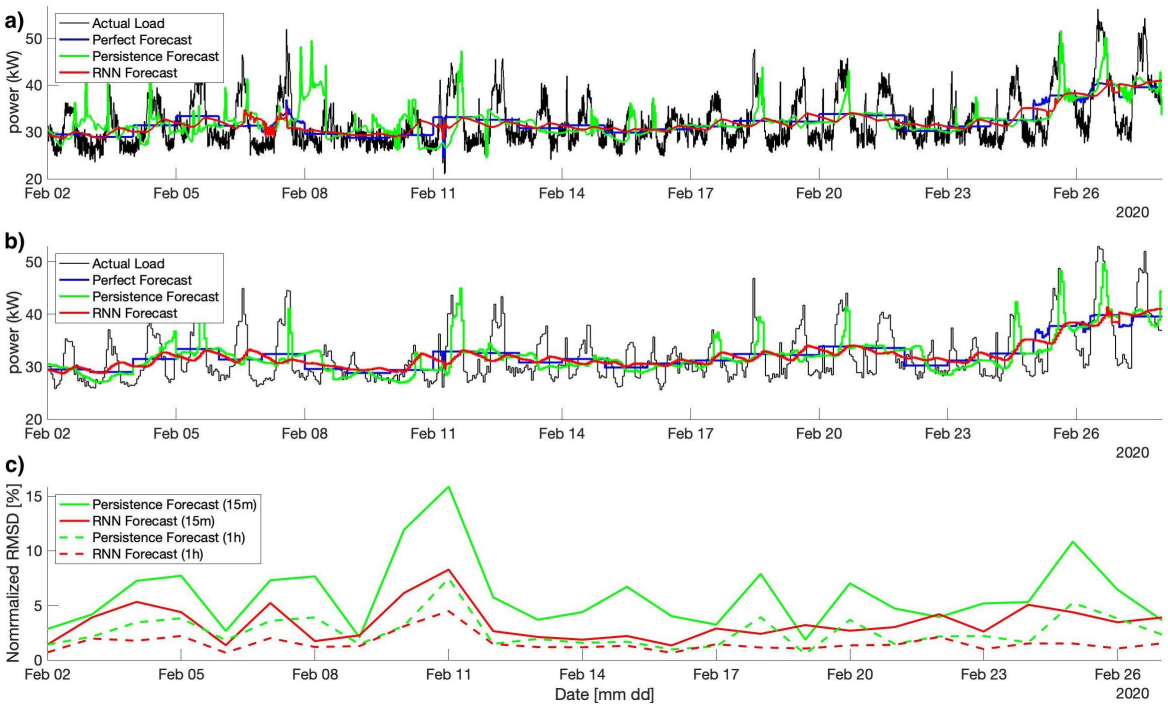

Figure 3.2. Monthly comparison of optimized net load for a) 15-min and b) 1-hour load profile; and c) nRMSD for RNN and persistence forecast scenarios with BESS c_p = 15 kW and c_e = 100 kWh.

3.2 Monthly results and statistics of load forecast error

We consider the three load forecasting scenarios (Section 2.2) for the month of February 2020. A sufficiently large battery capacity ($c_p = 15$ kW and $c_e = 100$ kWh) was selected to reduce the peak load to PP for perfect forecasts. While in practice demand charges are only assessed for the maximum load in the month, here we apply the optimization daily to test the ability to reduce peak loads for different load shapes and forecast errors. The day-by-day peak shaving performance comparison for both 15-min and 1-hour temporal load resolution is presented in Fig. 3.2a and Fig. 3.2b respectively. The optimized net load for perfect forecast is flat for most days. When the load is high (e.g. Feb 25 - 27), the battery capacity is insufficient to completely flatten the load.

When 24 hour persistence forecast errors are large and the forecast is too small (e.g. Feb

11 and Feb 25), the energy capacity of the battery is insufficient to flatten the load, resulting in large optimized net load. The optimized net load for Feb 11 is very large for persistence forecasts due to huge load variability compared to Feb 10. This verifies that the forecast error is a significant barrier to reducing peak load. The higher the forecast error, the larger is the deviation in optimized net load, resulting in higher optimal demand charge.

The RNN optimized net load is much higher than perfect forecasts due to load forecast error between the actual and predicted load, resulting in higher ODC. During days with small load (e.g., Feb 13 to 16), the battery capacity is sufficiently large to reduce the peak load to near the PP, yielding an almost flat net load for RNN forecast.

The normalized root mean square difference (nRMSD) for optimized net load for different forecast scenarios compared to the optimized net load with perfect forecast is shown in Fig. 3.2c. As persistence forecasts have the largest average load forecast error (nRMSD= 10.2%), the average 15 min and 1 hour nRMSD is found to be 5.64% and 2.94% respectively. The RNN forecasts outperform the 24 hour persistence forecasts on all days except Feb 19. RNN forecasts deliver a monthly nRMSD net load average of 3.49% and 1.58% for 15 min and 1 hour load resolution respectively, placing it approximately halfway between persistence and perfect forecasts. In general, this result confirms that the optimized net load can be reduced by RNN forecasts. The RNN optimized net load is not flat as the MPC algorithm is based on the forecasted load. For example, if RNN forecast is much higher compared to the actual load during the morning, the MPC will import more power from the grid and charge the BESS, causing higher ODC.

The average nRMSD for the 1 hour optimized net load is smaller compared to the 15 min load resolution. This result verifies that the ODC is underestimated by the low resolution load profile, due to load averaging of the 15 min load profile.

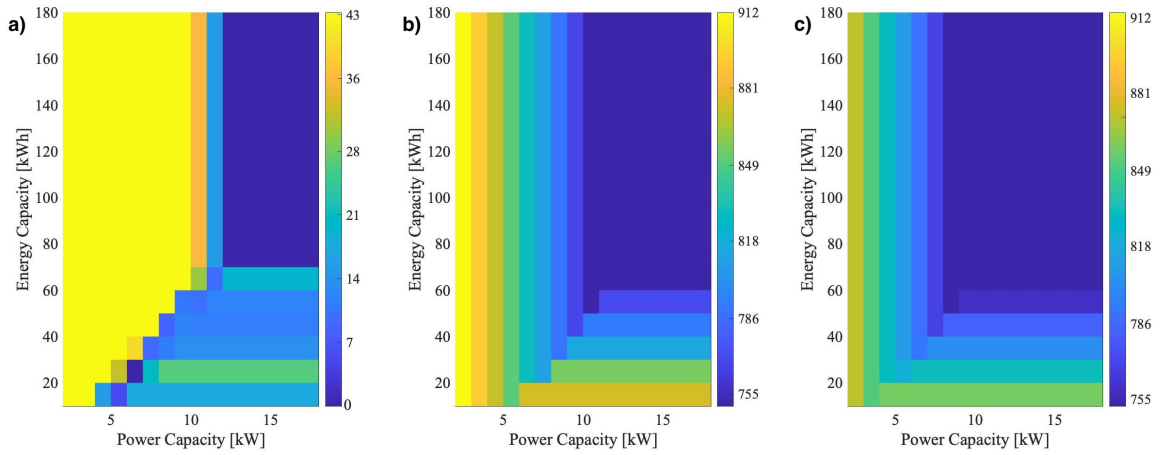

Figure 3.3. Demand charge metrics ($, color) for Feb 12 as a function of power and energy capacity: (a) DODC, (b) ODC_{15-min}, and (c) ODC_{1-hour}

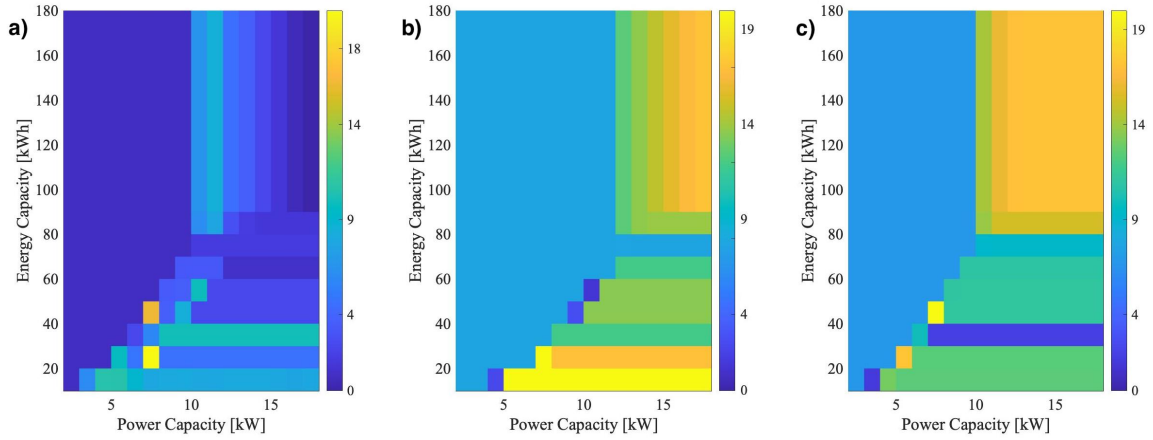

Figure 3.4. Comparison of demand charge metrics ($, color) when BESS is operated without MPC algorithm and with MPC algorithm for RNN forecast: (a) DODC, (b) ODC_{15-min}, and (c) ODC_{1-hour} as a function of power and energy capacity for Feb 12

3.3 Battery rating space analysis

3.3.1 Overview

The ODC depends on the BESS energy and power capacities. The ODC for 15 min (ODC_{15-min}) and 1 hour (ODC_{1-hour}) temporal resolution is plotted in Fig. 3.3b and Fig. 3.3c respectively across the battery rating space based on the RNN forecasts on Feb 11. We observe that the ODC is inversely proportional to BESS power and energy capacities. The difference between the two corresponding ODCs (DODC) is plotted in Fig. 3.3a. The battery rating space is divided into three regions based on the distribution of DODC in Fig. 3.3a. In the optimal region, the demand charges for both temporal resolutions are the same (i.e. $711.7), resulting in zero DODC values. Any additional BESS capacity is unable to reduce the optimized peak load below PP i.e. 32.77 kW or $675.7 demand charge, for both load resolutions. In Fig. 3.3b and c, we observed that the net load optimized by the BESS in the optimal region are identical for both load profiles resulting in zero DODC. But the ODC is higher compared to perfect forecast. This is due to the difference between the RNN forecasted load and the actual load during the initial time period of the day. As the BESS charging/discharging decision is based on load forecasts, the grid import is slightly higher than PP. This phenomenon is analyzed in more detail in 3.3.2. The rest of the battery space is split into the power-constrained and energy-constrained regions.

The MPC algorithm optimizes BESS dispatch in Step 4 to mitigate net load deviations caused due to forecast errors. The optimal demand charge for 15 min and 1 hour resolution has been compared with a BESS charged/discharged without and with MPC, as shown in Fig. 3.4b and Fig. 3.4c. In the optimal region, both (ODC_{15-min}) and (ODC_{1-hour}) is $17.15 less when the battery is charged/discharged based on MPC. Similar results have been confirmed for both power and energy constrained regions. The short-term load forecast error reduces as it gets updated at every time interval when using MPC resulting in reduced optimized net load. Therefore, we can conclude that the MPC controller optimizes BESS dispatch scheduling and can reduce peak load with lesser BESS capacity.

3.3.2 Power-constrained region

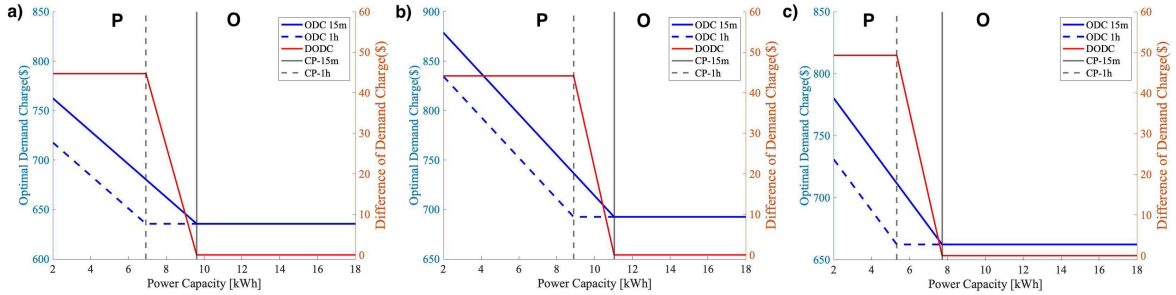

Figure 3.5. DODC, $\text{ODC}_{15-\text{min}}$, and $\text{ODC}_{1-\text{hour}}$ on Feb 13 at a fixed BESS energy capacity of 150 kWh for a) perfect b) persistence and c) RNN forecast. O represents the optimal region and P represents the power-constrained region. The vertical grey lines represent critical power (CP).

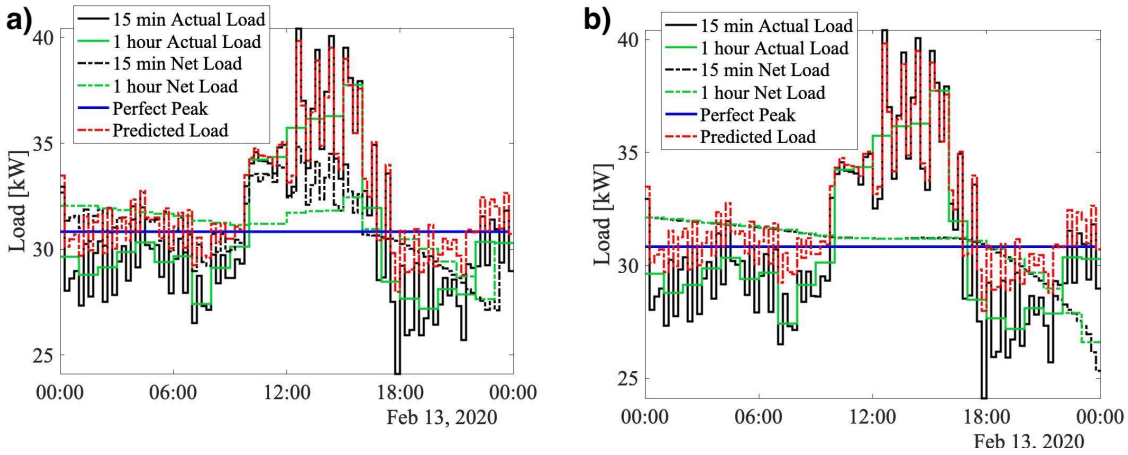

Figure 3.6. 15-min and 1-hour optimized net load by the following BESS: a) $c_p = 5.0$ kW, $c_e = 150$ kWh; b) $c_p = 7.7$ kW, $c_e = 150$ kWh on Feb 13.

To analyse the power-constrained region, the energy capacity of the battery is fixed at 150 kWh, which is higher than the critical energy (CE) of the load profile for February 13 (68.07 kWh). Fig. 3.5a shows that the ODC for both 15 min and 1 hour resolutions decrease linearly starting from \$712.22 and \$668.92 respectively and in parallel with a fixed DODC of \$43.30 for perfect forecast, until they reach the same value (\$635.59) after reaching the CP of the load. A similar trend is observed for both persistence and RNN forecasts in Fig. 3.5b and Fig. 3.5c respectively. Compared to the perfect forecast, the RNN forecast has a higher ODC

for both 15 min ($780.22) and 1 hour ($730.96) temporal resolutions in the power constrained region (P in Fig. 3.5c) due to the significant error (nRMSD= 4.77%) in predicted load and actual load during the day. The ODC is even higher for the persistence forecast than the perfect and RNN forecasts due to higher average load error (nRMSD= 9.58%).

The battery rating space is divided into two regions based on DODC, i.e. the power-constrained region (P) and the optimal region (O). CP_{15-min} and CP_{1-hour} of the predicted load describes the transient zone between the power-constrained and optimal region. The transient zone based on the RNN forecast (Fig. 3.5c) is smaller than for the persistence forecast as the CP for predicted load is lesser compared to CP for persistence load. So the optimal region starts at $CP_{15-min} = 7.71$kW and $CP_{15-min} = 11.10$kW for the RNN and persistence forecasts, respectively.

To further analyze the effect of RNN load forecast error on the two battery space regions, the optimization results of BESS with power capacity of 5 kW (power-constrained region) and 7.71 kW $= CP_{15-min}$ (optimal region) are shown in Fig. 3.6a and Fig. 3.6b respectively for a constant battery energy capacity $c_e = 150$ kWh. The optimized net load by the BESS is affected by time averaging of the load profile from high resolution (15 min) to low resolution (1 hour). In Fig. 3.6a, the peak net load occurs during the time interval of 12:30-12:45 h (34.83 kW) and 15:00-16:00 h (32.44 kW) respectively. This results in DODC = $49.26 due to a constant net load difference of 2.39 kW throughout the power-constrained region. When the power capacity increases to 7.71 kW i.e. CP of the predicted load, the DODC becomes zero, i.e. the net optimized load for both temporal resolutions are identical (Fig. 3.6b). However the net load imported from the grid is much higher compared to PP (blue line in Fig. 3.6b) resulting in higher ODC even with sufficient battery power capacity. As the predicted load (red line) during 00:15-09:30 h is much higher than the actual load (black line), the grid import during this time interval is higher than PP due to charging of the battery. Due to excess charging of the battery during the day, the battery gets discharged during the evening (18:00-23:45 h) to maintain the battery SOC at 0.5 even though there are no ODC benefits. Therefore, the ODC

depends significantly on the accuracy of the load forecasting model. As the persistence forecast has lower accuracy, it results in higher $\text{ODC}_{15-\text{min}}$, and $\text{ODC}_{1-\text{hour}}$ than RNN forecast.

3.3.3 Energy-constrained Region

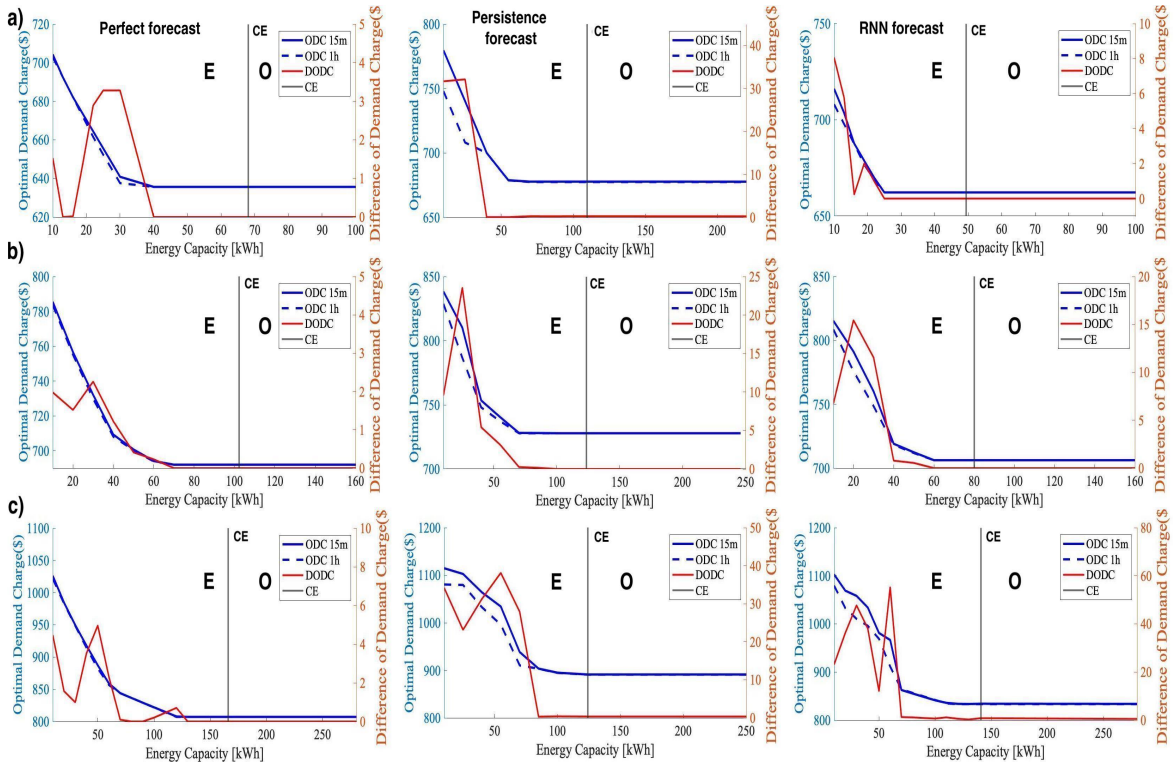

Figure 3.7. DODC, $\text{ODC}_{15-\text{min}}$, and $\text{ODC}_{1-\text{hour}}$ at CP on a) Feb 13, b) Feb 21, and c) Feb 26 for perfect (first column), persistence (second column) and RNN (third column) forecasts, respectively. O represents the optimal region and E represents the energy-constrained region.

In this section, we investigate the energy-constrained region by setting the BESS power capacity to CP such that the power capacity has no significant impact on peak shaving. The variation of DODC, $\text{ODC}_{15-\text{min}}$, and $\text{ODC}_{1-\text{hour}}$ at CP on three different days (Feb 13, 21, and 26) is presented in Fig. 3.7a, Fig. 3.7b and Fig. 3.7c respectively for perfect, persistence, and RNN forecasts. The left part in each figure represents the energy-constrained region (E) whereas the right part is the optimal region (O), separated by the critical energy (CE) line. Even if the energy capacity is constrained, i.e. c_eCE, the ODC for both load profiles are closer to each

other than in the power-constrained region, resulting in a lower magnitude of DODC. Although the variation in DODC is irregular, it shows a decreasing trend until it reaches zero below CE. Similar to the results observed in the power-constrained region, the ODC for both 15 min and 1 hour resolution for RNN forecast are higher than for the perfect forecast, but lower than for the persistence forecast. The results in Fig. 3.7a further show that the BESS is unable to reach PP in the optimal region due to load forecasting errors in real-time. We also notice that the DODC becomes zero for $c_e >$ CE for all three forecasts. The same phenomenon is observed in Fig. 3.7b and Fig. 3.7c for Feb 21 and Feb 26, respectively but the distribution of zero DODC differs greatly. This is due to the change in peak period duration of some load profiles after time-averaging, as explained by Liu et al. [22].

3.3.4 Discussion

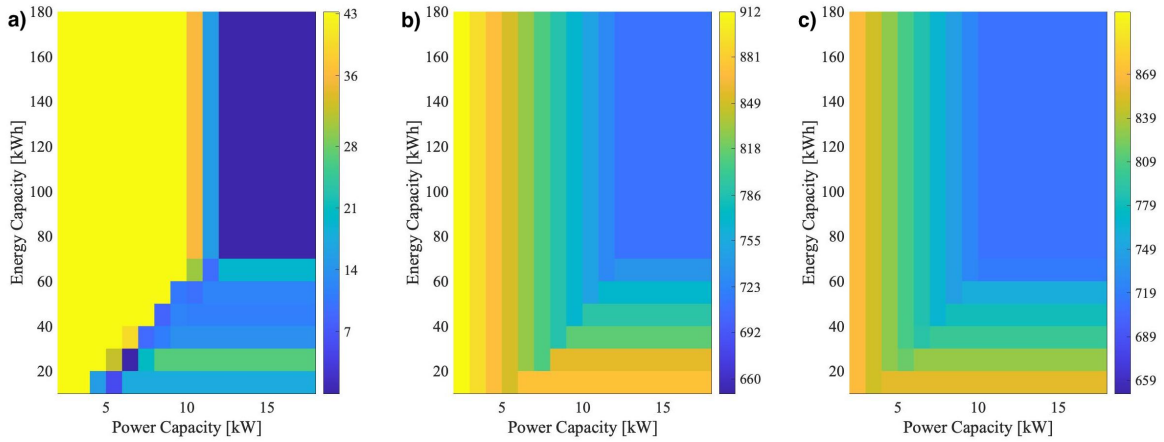

Figure 3.8. Average demand charge metrics ($, color) for the month of February as a function of power and energy capacity: (a) DODC, (b) $\text{ODC}_{15-\text{min}}$, and (c) $\text{ODC}_{1-\text{hour}}$

Load forecast errors cause a significant deviation between realistic peak shaving and ideal peak shaving. For perfect forecast, Liu et al. [22] concluded that the optimal demand charge for 15 min temporal resolution is higher compared to 1 hour resolution in both power and energy constrained regions. A similar result was observed for RNN load forecasting, but the ODC for both temporal resolution is higher compared to perfect forecast (refer Sec. 3.3). The monthly net

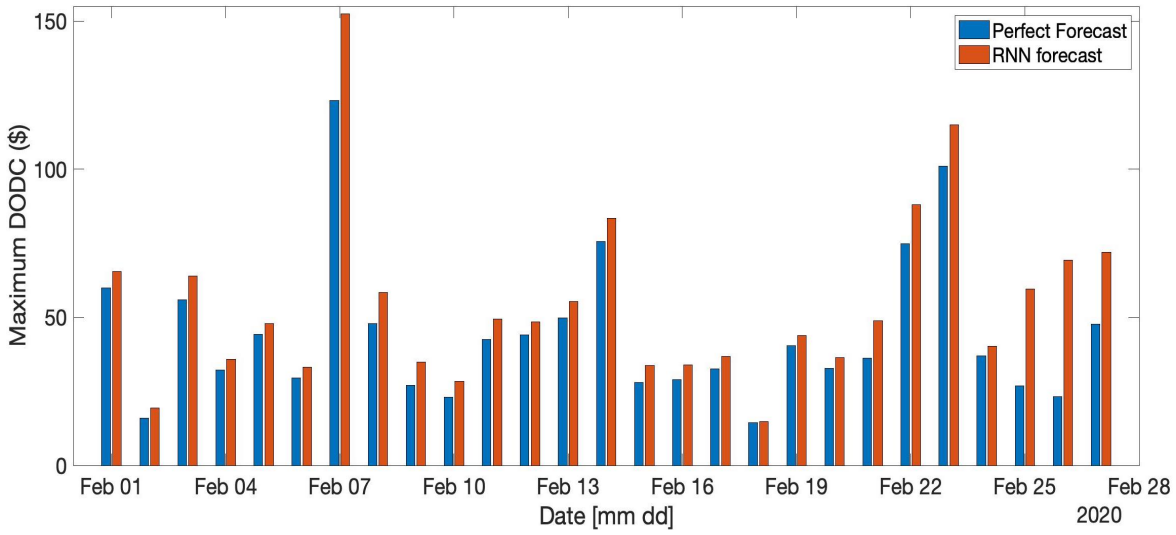

Figure 3.9. Maximum DODC ($) for perfect and RNN forecast during the month of February

load results in Section 3.2 verify that the forecast error plays a significant role in the optimized net load variability. For example, in Fig. 3.6b, the optimized net load with RNN forecast is much higher than PP even with sufficient BESS capacity, due to load forecast errors. Although the DODC is zero in the optimal region, the ODC for RNN forecast is higher than perfect forecasts.

The results from Sec.3.3 are expanded for demand charge analysis of a month. The average DODC, $\text{ODC}_{15-\text{min}}$ and $\text{ODC}_{1-\text{hour}}$ for the whole battery space during the month of February is plotted in Fig. 3.8. Furthermore, the maximum DODC for each day during the month of February for perfect and RNN forecasts are shown in Fig. 3.9. We observe that the DODC is higher for days when there is a large variation in the load profile. When the 15 min load profile is averaged to 1 hour temporal resolution, the peak load during the day reduces significantly resulting in higher DODC. The results for RNN forecasts suggest that DODC is higher compared to perfect forecasts as 15 min load forecast errors are higher compared to 1 hour loads.

The demand charge reduction by the BESS over a month depends on the daily load profile of the month with the largest CP or CE. The load profiles for a particular month can be classified into two types: (a) ”spiky” peak load profile due to high CP and low CE (e.g. Feb 12); (b) ”broad” peak load profile caused due to low CP and high CE (e.g. Feb 26). A power-constrained

BESS will significantly overestimate ODC for a ”spiky” load profile. Similarly, the DODC for energy-constrained BESS will be higher for ”broad” peak load profiles (refer 3.7c for RNN forecast). As the demand charges are calculated based on the peak load for a whole month, the BESS capacity must be selected based on the days having largest CP and CE.

Chapter 4

CONCLUSIONS

In this paper, we developed a linear programming routine to optimize the battery energy storage system (BESS) dispatch schedule based on a model predictive control (MPC) algorithm, that leverages load predictions to reduce building peak demand. The MPC controller optimizes the BESS charging decisions based on more accurate short-term forecast inputs at every time interval, which further reduces the net load variability and corresponding optimal demand charge. The linear optimization framework that integrates load forecasts and MPC allows a more realistic study of the effect of temporal resolution in peak shaving and its relationship with BESS capacities. We demonstrated the optimized dispatch for operational demand charge management using one month of real data. This study differs from the literature regarding the forecast error modeling as we use actual load forecasts instead of perfect forecasts. We generated load forecasts using a recurrent neural network (RNN) forecasting model with one year of historical data. A simple corrective deterministic strategy is applied to reduce negative consequences (load peaks) of forecast errors. The optimized net load for RNN forecast is compared with results from persistence and perfect forecasts. We conclude that the optimal demand charge for RNN forecast is much higher compared to perfect forecast for a fixed BESS capacity. However, it is much lower than persistence forecast due to lower deviations in predicted load than persistence load.

We have also studied the effect of temporal load resolution on peak shaving to understand the intrinsic properties of load profiles and their relationships with BESS ratings. Our results

show that the low resolution load underestimates the optimal demand charge (ODC) by 6.31% or $49.26 for RNN forecasted loads when the BESS power capacity is constrained. We have partitioned the BESS ratings space into different regions based on the battery power and energy capacity to study BESS demand charge management at different temporal resolution. The 15 min and 1 hour ODC is 8.71% and 8.48% higher respectively for RNN forecasts than perfect forecasts in the power. Large forecast errors (4.77%) results in higher charging of the battery during the day that increases the peak demand. As a result the optimized net load for RNN forecast is higher than perfect peak resulting in higher ODC even though the DODC is equal to zero in the optimal region for all load forecasts. The forecast errors tend to increase the 15 min load variability more than 1 hour load time-series. Therefore, it is critical to oversize BESS capacities determined from 1 hour resolution modeling to mitigate the errors in demand charge savings estimation caused due to load resolution conversion. Conversely, high-resolution load profiles are required to capture actual peak demand for a BESS having limited capacities. A given BESS may behave as power-constrained during months with broad daily load peaks and energy-constrained during months with spiky load characteristics.

The thesis is currently being prepared for submission for publication of the material. Roy, Rahul; Silwal, Sushil; Kleissl, Jan. The thesis author was the primary investigator and author of this material. I would like to acknowledge Dr. Sushil Silwal and Prof. Jan Kleissl for their valuable support of the research work.

Bibliography

[1] Tobias Beck, Hendrik Kondziella, Guillaume Huard, and Thomas Bruckner. Assessing the influence of the temporal resolution of electrical load and pv generation profiles on self-consumption and sizing of pv-battery systems. *Applied energy*, 173:331–342, 2016.

[2] Valentin Bertsch, Jutta Geldermann, and Tobias Lühn. What drives the profitability of household pv investments, self-consumption and self-sufficiency? *Applied Energy*, 204:1–15, 2017.

[3] Felix Braam, Raphael Hollinger, Martin Llerena Engesser, Stine Müller, Robert Kohrs, and Christof Wittwer. Peak shaving with photovoltaic-battery systems. In *IEEE PES Innovative Smart Grid Technologies, Europe*, pages 1–5. IEEE, 2014.

[4] Alessandro Burgio, Daniele Menniti, Nicola Sorrentino, Anna Pinnarelli, and Zbigniew Leonowicz. Influence and impact of data averaging and temporal resolution on the assessment of energetic, economic and technical issues of hybrid photovoltaic-battery systems. *Energies*, 13(2):354, 2020.

[5] Sunliang Cao and Kai Sirén. Impact of simulation time-resolution on the matching of pv production and household electric demand. *Applied Energy*, 128:192–208, 2014.

[6] Kein Huat Chua, Yun Seng Lim, and Stella Morris. Battery energy storage system for peak shaving and voltage unbalance mitigation. *International Journal of Smart Grid and Clean Energy*, 2(3):357–363, 2013.

[7] Kein Huat Chua, Yun Seng Lim, and Stella Morris. Energy storage system for peak shaving. *International Journal of Energy Sector Management*, 2016.

[8] Cédric Clastres, TT Ha Pham, F Wurtz, and S Bacha. Optimal household energy management and participation in ancillary services with pv production. *Energy*, 35(1):55–64, 2010.

[9] Jackravut Dejvises. Energy storage system sizing for peak shaving in thailand. *ECTI Transactions on Electrical Engineering, Electronics, and Communications*, 14(1):49–55, 2016.

[10] R Hanna, J Kleissl, A Nottrott, and M Ferry. Energy dispatch schedule optimization for demand charge reduction using a photovoltaic-battery storage system with solar forecasting. *Solar Energy*, 103:269–287, 2014.

[11] Abubakar Sani Hassan, Liana Cipcigan, and Nick Jenkins. Optimal battery storage operation for pv systems with tariff incentives. *Applied Energy*, 203:422–441, 2017.

[12] Eric Hoevenaars. *Temporal resolution in time series and probabilistic models of renewable power systems*. University of Victoria (Canada), 2012.

[13] Majid Hosseina and Seyed Mohammad Taghi Bathaee. Optimal scheduling for distribution network with redox flow battery storage. *Energy conversion and management*, 121:145–151, 2016.

[14] Bwo-Ren Ke, Te-Tien Ku, Yu-Lung Ke, Chen-Yuan Chuang, and Hong-Zhang Chen. Sizing the battery energy storage system on a university campus with prediction of load and photovoltaic generation. *IEEE Transactions on Industry Applications*, 52(2):1136–1147, 2015.

[15] Thongchart Kerdphol, Kiyotaka Fuji, Yasunori Mitani, Masayuki Watanabe, and Yaser Qudaih. Optimization of a battery energy storage system using particle swarm optimization for stand-alone microgrids. *International Journal of Electrical Power & Energy Systems*, 81:32–39, 2016.

[16] Rakkyung Ko, Seongbae Kong, and Sung-Kwan Joo. Mixed integer programming (mip)-based energy storage system scheduling method for reducing the electricity purchasing cost in an urban railroad system. *The Transactions of the Korean Institute of Electrical Engineers*, 64(7):1125–1129, 2015.

[17] Michael Koller, Theodor Borsche, Andreas Ulbig, and Göran Andersson. Defining a degradation cost function for optimal control of a battery energy storage system. In *2013 IEEE Grenoble Conference*, pages 1–6. IEEE, 2013.

[18] Olga Lavrova, Feng Cheng, Sh Abdollahy, H Barsun, A Mammoli, D Dreisigmayer, Steve Willard, Brian Arellano, and C Van Zeyl. Analysis of battery storage utilization for load shifting and peak smoothing on a distribution feeder in new mexico. In *2012 IEEE PES Innovative Smart Grid Technologies (ISGT)*, pages 1–6. IEEE, 2012.

[19] Jason Leadbetter and Lukas Swan. Battery storage system for residential electricity peak demand shaving. *Energy and buildings*, 55:685–692, 2012.

[20] Jason Leadbetter and Lukas G Swan. Selection of battery technology to support grid-integrated renewable electricity. *Journal of Power Sources*, 216:376–386, 2012.

[21] Jochen Linssen, Peter Stenzel, and Johannes Fleer. Techno-economic analysis of photovoltaic battery systems and the influence of different consumer load profiles. *Applied Energy*, 185:2019–2025, 2017.

[22] Shiyi Liu, Sushil Silwal, and Jan Kleissl. Power and energy constrained battery operating regimes: Effect of temporal resolution on peak shaving by battery energy storage systems. *Journal of Renewable and Sustainable Energy*, 2021.

[23] Chao Lu, Hanchen Xu, Xin Pan, and Jie Song. Optimal sizing and control of battery energy storage system for peak load shaving. *Energies*, 7(12):8396–8410, 2014.

[24] Alexandre Lucas and Stamatios Chondrogiannis. Smart grid energy storage controller for frequency regulation and peak shaving, using a vanadium redox flow battery. *International Journal of Electrical Power & Energy Systems*, 80:26–36, 2016.

[25] Aravind P Manjunatha, Petr Korba, and Vanessa Stauch. Integration of large battery storage system into distribution grid with renewable generation. In *2013 IEEE Grenoble Conference*, pages 1–6. IEEE, 2013.

[26] E Matallanas, Manuel Castillo-Cagigal, A Gutiérrez, F Monasterio-Huelin, Estefanía Caamaño-Martín, D Masa, and J Jiménez-Leube. Neural network controller for active demand-side management with pv energy in the residential sector. *Applied Energy*, 91(1):90–97, 2012.

[27] Mahdi Motalleb, Ehsan Reihani, and Reza Ghorbani. Optimal placement and sizing of the storage supporting transmission and distribution networks. *Renewable Energy*, 94:651–659, 2016.

[28] Maik Naumann, Ralph Ch Karl, Cong Nam Truong, Andreas Jossen, and Holger C Hesse. Lithium-ion battery cost analysis in pv-household application. *Energy Procedia*, 73:37–47, 2015.

[29] A Nottrott, Jan Kleissl, and Byron Washom. Energy dispatch schedule optimization and cost benefit analysis for grid-connected, photovoltaic-battery storage systems. *Renewable Energy*, 55:230–240, 2013.

[30] Balint D Olaszi and Jozsef Ladanyi. Comparison of different discharge strategies of grid-connected residential pv systems with energy storage in perspective of optimal battery energy storage system sizing. *Renewable and Sustainable Energy Reviews*, 75:710–718, 2017.

[31] Alexandre Oudalov, Rachid Cherkaoui, and Antoine Beguin. Sizing and optimal operation of battery energy storage system for peak shaving application. In *2007 IEEE Lausanne Power Tech*, pages 621–625. IEEE, 2007.

[32] Alessandra Parisio, Evangelos Rikos, George Tzamalis, and Luigi Glielmo. Use of model predictive control for experimental microgrid optimization. *Applied Energy*, 115:37–46, 2014.

[33] TT Ha Pham, Frédéric Wurtz, and Seddik Bacha. Optimal operation of a pv based multi-source system and energy management for household application. In *2009 IEEE International Conference on Industrial Technology*, pages 1–5. IEEE, 2009.

[34] Azar Rahimi, M Zarghami, M Vaziri, and S Vadhva. A simple and effective approach for peak load shaving using battery storage systems. In *2013 North American Power Symposium (NAPS)*, pages 1–5. IEEE, 2013.

[35] Ehsan Reihani, Mahdi Motalleb, Reza Ghorbani, and Lyes Saad Saoud. Load peak shaving and power smoothing of a distribution grid with high renewable energy penetration. *Renewable energy*, 86:1372–1379, 2016.

[36] Yann Riffonneau, Seddik Bacha, Franck Barruel, and Stephane Ploix. Optimal power flow management for grid connected pv systems with batteries. *IEEE Transactions on sustainable energy*, 2(3):309–320, 2011.

[37] Peter Stenzel, Jochen Linssen, Johannes Fleer, and Florian Busch. Impact of temporal resolution of supply and demand profiles on the design of photovoltaic battery systems for increased self-consumption. In *2016 IEEE International Energy Conference (ENERGYCON)*, pages 1–6. IEEE, 2016.

[38] Enrico Telaretti and Luigi Dusonchet. Battery storage systems for peak load shaving applications: Part 2: Economic feasibility and sensitivity analysis. In *2016 IEEE 16th International Conference on Environment and Electrical Engineering (EEEIC)*, pages 1–6. IEEE, 2016.

[39] Fei Teng, Danny Pudjianto, Goran Strbac, Nigel Brandon, Alan Thomson, and John Miles. Potential value of energy storage in the uk electricity system. *Proceedings of the Institution of Civil Engineers-Energy*, 168(2):107–117, 2015.

[40] Thijs Van der Klauw, Johann L Hurink, and Gerard JM Smit. Scheduling of electricity storage for peak shaving with minimal device wear. *Energies*, 9(6):465, 2016.

[41] Chandu Venu, Yann Riffonneau, Seddik Bacha, and Yahia Baghzouz. Battery storage system sizing in distribution feeders with distributed photovoltaic systems. In *2009 IEEE Bucharest PowerTech*, pages 1–5. IEEE, 2009.

[42] Zhou Wu, Henerica Tazvinga, and Xiaohua Xia. Demand side management of photovoltaic-battery hybrid system. *Applied Energy*, 148:294–304, 2015.

[43] Nicolas Wyrsch, Yannick Riesen, and Christophe Ballif. Effect of the fluctuations of pv production and electricity demand on the pv electricity self-consumption. In *Proceedings of the 28th European Photovoltaic Solar Energy Conference and Exhibition*, number CONF, pages 4322–4324, 2013.

[44] Alexander Zeh and Rolf Witzmann. Operational strategies for battery storage systems in low-voltage distribution grids to limit the feed-in power of roof-mounted solar power systems. *Energy Procedia*, 46:114–123, 2014.

[45] Yan Zhang, Baolong Liu, Tao Zhang, and Bo Guo. An intelligent control strategy of battery energy storage system for microgrid energy management under forecast uncertainties. *Int. J. Electrochem. Sci*, 9(8):4190–4204, 2014.

[46] Yan Zhang, Tao Zhang, Rui Wang, Yajie Liu, and Bo Guo. Optimal operation of a smart residential microgrid based on model predictive control by considering uncertainties and storage impacts. *Solar Energy*, 122:1052–1065, 2015.

[47] Menglian Zheng, Christoph J Meinrenken, and Klaus S Lackner. Smart households: Dispatch strategies and economic analysis of distributed energy storage for residential peak shaving. *Applied Energy*, 147:246–257, 2015.